

ORIGINAL ARTICLE



3D-Printing with steel of a bolted connection

Maren Erven, Jörg Lange, Thilo Feucht

Correspondence

Maren Erven, M. Sc.
Technical University of Darmstadt
Steel Construction
Franziska-Braun-Straße 3
64287 Darmstadt
Germany
erven@stahlbau.tu-darmstadt.de

Abstract

Additive Manufacturing seems promising for the steel construction industry, especially for small components with complex shapes. With Wire-and-Arc-Additive-Manufacturing (WAAM) a process was found which is fast and cheap compared to other Additive Manufacturing processes for metals. Furthermore, arc-welding is well known in steel construction industry.

Bolted head plates are a common connection. Although they are relatively easy to produce, they are uneconomical in load transfer due to straining of the plates which are subject to bending. This type of connection is predestined for Additive Manufacturing. Rethinking the structure by taking into account the potentials of Additive Manufacturing brings a clear advantage compared to the conventional production. Thus, with a material saving of 60 % the same load capacity of the original flat head plate can be achieved.

The paper shows how the new production process WAAM can significantly change the shape of structures on the example of a bolted head plate. Therefore, all steps from the original design to the manufactured structure are demonstrated, including the structure finding by using topology optimization, the manufacturing with different parameters and a first testing of the manufactured structures.

Keywords

Additive Manufacturing, Topology Optimization, Connections, Fabrication and Construction, Innovative Structures

1 Introduction

3D-Printing or Additive Manufacturing (AM) is, in most cases, the process of adding material layer by layer to build a structure. Some exceptions do exist, such as the use of holographic to 3D-print an object in one step [1]. Nonetheless, Additive Manufacturing is different from the conventional subtractive manufacturing processes (like milling, drilling ...). With the progress in technology it is now possible to print nearly every material. Therefore, AM is becoming more and more popular in the building construction industry [2, 3].

In general, advantages of AM can be described as follows [4]:

- Function-oriented, individual design of the component,
- Avoidance of production-ready design, taking into account process-related constraints (e.g. cast components, avoidance of undercuts, overhangs, cavities, etc.),
- No need for formwork and tools,
- Reduction of waste.

However, there also some disadvantages [4]:

- Investment in new machines,
- Unknown material properties and behaviour,
- Time consuming manufacturing processes.

At the department of civil engineering of TU Darmstadt the different materials applicable for construction industry and their potentials are investigated.

According to the factors mentioned above, especially small components with complex shapes or freeform components for architectural reasons seem promising [5, 6].

2 Additive Manufacturing with steel

For printing metal different processes are applicable. In order to achieve a homogeneous and stable product energy is essential to form the solid printing material and join the 3D-printed layers. Depending on type of printing material and source of energy the different processes can be classified (see Figure 1).

2.1 Process comparison

An AM process suitable for steel construction should take into account the factors for the successful project planning of a building (quality, deadlines and costs). Accordingly, it should provide suitable material properties and fast production rates as well as low material consumption and costs.

For foil-shaped starting materials high material and time consumption are to be regarded as disadvantageous [4]. Furthermore, the size of the additively manufactured structures is limited by the size of the film. The same problems are encountered with powder bed processes [7].

	WIRE	POWDER BED	POWDER DEPOSITION	FOIL
LASER	LMD, DMD	SLS, DMLS, SLM, LBM, DMP, LMF	LENS, LMD, LPD, LRM, LPmD	
BEAM	EBF ³ , EBAM	EBS, EBM	EBAM	
ARC	WAAM			
BINDER		3DP		LOM, LLM, SHEET LAMINATION

Figure 1 Different processes of 3D-metal-printing divided by type of starting material and energy source/glue

The advantage of powder deposition and wire-based processes is that only needed material is utilized. In contrast to the powder bed process, no container is required in which the component is produced. Therefore, the size of the finished component is not limited [8]. The disadvantage of a powdered starting material is the need for special work safety measures. The problem with wire-based processes, however, is the inaccuracy of the final contour [7, 8].

As a technical process, both binder and sintering have to be critically evaluated in terms of quality [4]. Melting is preferable to sintering due to the higher density of the resulting structure. With regard to the effort required, the electron beam as an energy source is to be evaluated poorly, since a vacuum chamber is necessary for precise production.

For steel construction, the advantages of wire-based arc welding (WAAM) are predominant, as small dimensions of less than one millimetre are of no significance. More importantly, production rates of up to 10 kg/h have already been achieved in high-speed processes and the technology is inexpensive and well-known [9–12].

2.2 WAAM

Arc welding is a classical fusion welding process. By utilizing an arc as thermal energy the filler wire is melted. It can be assumed that a large energy per unit length (as proportional to the energy applied) leads to high temperatures in the weld bead. These high temperatures lead to melting and thus to an inaccurate contour. Furthermore, the material properties depend on the energy per unit length. In general, it can be seen that a low energy per unit length is more advantageous for the material properties. Research is therefore interested in reducing the energy input into the weld seam as far as possible in order to limit negative effects [13].

Although MX3D from the Netherlands shows that it is also possible to print 3D with a normal welding process [14, 15], there are some specialized heat-reduced (cold) processes that facilitate production. As experimental setup the “CMT Cycle Step” process developed by Fronius is used at the TU Darmstadt. In this process, the wire is mechanically retracted after the drop separation, allowing for the drop to have a defined shape and time to cool down [16–20].

2.3 Geometrical limitations

For designing a 3D-printed structure it is necessary to know the geometric limits of Additive Manufacturing. For this purpose literature values were used. A minimum width of 2.5 mm is assumed [21]. A further parameter of the geometric boundary conditions is the manufacturing in constrained positions, here constrained positions up to 40° are assumed to be possible [13].

For the production of the structure, parameter studies were carried out. Furthermore, the fabrication of a bridge on site in autumn 2019 on the premises of the TU Darmstadt has shown that it is also possible to print cantilevered horizontal structures [20, 22].

3 Head plate joint / beam splice

In steel construction, bolted head plates (like used in the beam splice in Figure 2 (left)) are a common connection, which is quite easy to produce. However the plate is subjected to bending which makes it less economical. A sufficient plate-thickness is required in order to transfer the bending moment. Furthermore, some areas, like the middle part of the plate, have only very little or no load at all. The mechanical T-stub model of the tensile zone has been investigated, applied and modified for over 50 years [23, 24]. Today's standardized concept combines the various investigations and current knowledge [25, 26].

3.1 Object of investigation

The paper focusses on the tensile zone of a beam splice for the outer row of bolts. As a simplification a possible shear force is neglected. The bolts will only be loaded in tension, shear is not considered. The dimension of the plate is chosen in such a way that the plate will fail under bending. The aim should be that the investigated FE model and the actual dimensions of the connection are approximately the same. Thus the FE model can provide a good approximation. Furthermore, the second row of bolts has approximately the same distance from the flange like the first. Provided that the positive effect of the web is not considered, the optimization can also be used for the second (inner) row of bolts. This can be compared with the simplified calculation according to EN 1993-1-8 6.2.7.1 [25]. The investigated area is shown in blue in Figure 2 (right).

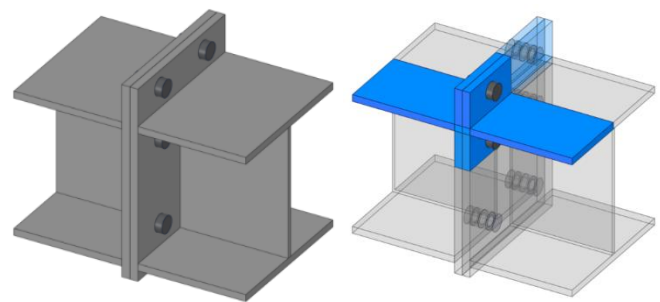


Figure 2 Head plate joint and area investigated (blue)

The FE model is limited to the T-stub area of the head plate. Instead of modelling the bolts they are represented by bearings. According to EN 1993-1-8 figure 6.2, the distance between flange and bolt in the T-stub model is reduced using the term $0,8 \cdot a \cdot \sqrt{2}$ [25]. This takes into account the load introduction via the weld seam. Due to Additive Manufacturing, the weld is omitted for form finding. This is the first material saving possibility by Additive Manufacturing.

3.2 Form finding by using topology optimization

To find a new structure topology optimization, one of the three common categories of structural optimization [27] was used. The optimization was done using Ansys Workbench. With the SIMP approach ("Solid Isotropic Material with Penalization") voids are inserted for unused, material-wasting areas of the structure. The approach assigns only one variable to each element: the ratio of the momentary density and the initial density [28].

As the minimum compliance describes the sum of the work caused by the element displacement over all the elements, it gives conclusions about the stiffness of the component. Therefore, finding the minimum compliance is a suitable target function for optimization of structures [27]. It is logical that maximum stiffness is achieved if the volume remains the same and is not reduced at all. However, this trivial solution has no practical benefit, as the component would remain the same and no material-saving design would result. Therefore, a volume restriction was introduced: for a certain proportion of the initial volume the arrangement of elements with the minimum compliance must be found.

When using topology optimization for form finding, it must be noted that currently used algorithms do not represent non-linearity. Thus, neither plasticity, stability problems nor non-linear bearings may be considered. In addition, it should be noted that the result of one optimization run only gives the stiffest structure and no information on whether the output can withstand the applied load. A subsequent non-linear analysis of the found structure is therefore always necessary.

The workflow is shown in Figure 3. At first, the non-linear initial system was realistically modelled (A). The boundary conditions defined thereby were transferred to a linear system (B). The linear system was then optimized for different mass ratios (C). In a subsequent non-linear analysis, the payload of each optimized structure was determined (D).

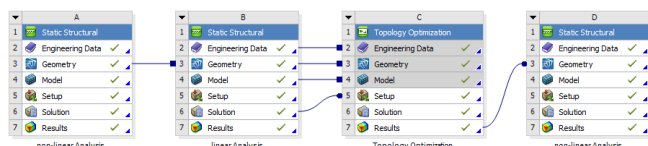


Figure 3 Optimization workflow for one mass restriction

3.3 Structural analysis

Figure 4 shows the von-Mises-equivalent stress and the deformation when reaching the load capacity according to mode 1 of the T-stub model. The yielded areas are located at the cut of the flange and at the area of the bolts. The resulting load is the reference for the optimization.

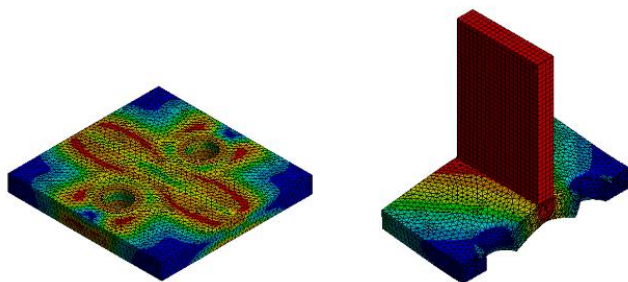


Figure 4 T-Stub under ultimate load von-Mises-Stress (left) and displacement (right)

For the analysis it was assumed that the additively produced structure will achieve the steel grade S 235. Likewise, stiffness and modulus of elasticity should be equal to "normal steel", as initial investigations show [21, 29]. For the load-bearing-analysis a non-linear-elastic material behaviour must be considered. The material properties are given in Table 1.

Table 1 Material behaviour for the different analyses

Material	Property	Symbol	Value
Linear-elastic-ideal-plastic	Linear-elastic	Density	ρ 7.850 kg/m ³
		Modulus of elasticity	E 210.000 MPa
		Poisson's ratio	ν 0,3
		Modulus of shear	G 80.769 MPa
	Yield strength	f_y 235 MPa	
	Tangent modulus of elasticity	E_T 0 MPa	

3.4 Topology optimization of the T-stub

In the next step, the system was transferred to a linear system for topology optimization. The topology optimization may only be carried out on the basis of a linear stress analysis, therefore the linear material properties are selected (see Table 1). The possibility of plasticizing the steel was not considered.

Compared to traditional manufacturing, Additive Manufacturing allows new (more complicated) geometries. Therefore, the thickness of the design space was increased by 100 mm compared to that of the original head plate to enable a more effective load introduction.

It should be noted that there must be sufficient space to tighten the bolt for subsequent assembly. A M20 bolt has a wrench size of 32 mm. A suitable wrench is available from an outer diameter of 49 mm. This cylinder was left out in the design space.

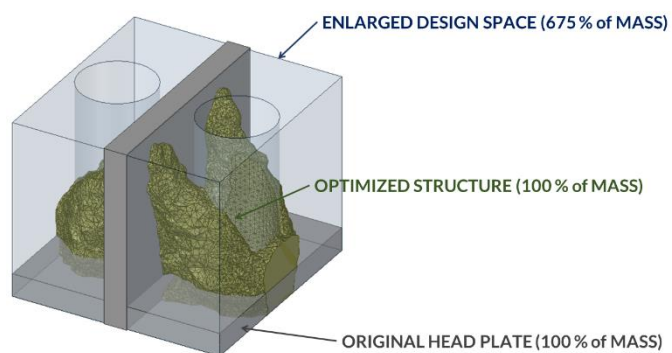


Figure 5 Comparison of original head plate, design space and optimized structure

Since the mass of the design space is much larger than that of the plate, a conversion of the masses from plate to block must be carried out (see Figure 5). The optimized geometries are examined for their load-bearing capacities in a subsequent non-linear analysis. The result in comparison to the original T-Stub is shown in Figure 6.

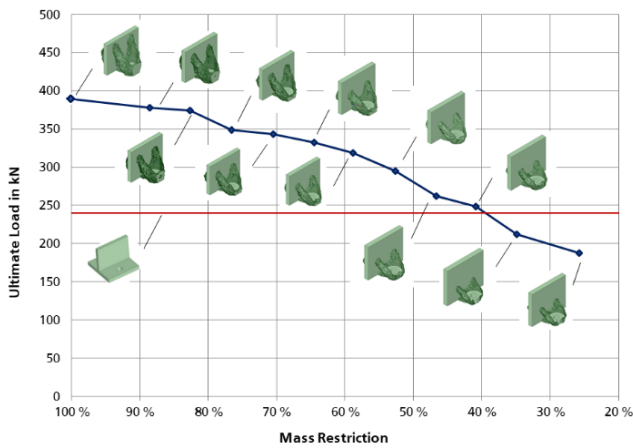


Figure 6 Load bearing capacity of different mass restrictions (blue) compared to the original design (red)

When comparing the optimized structures with the original plate it can be seen that two angled braces are formed along the flange. Furthermore, in the lower part of the flange there is always a part still connected. This area serves to absorb the compressive forces, whereas the braces forming upwards are supposed to absorb the tensile forces. This behaviour can be roughly described as a simple truss model (Figure 7 right). The assumption that tension and compression struts are formed is confirmed by a stress analysis. Figure 7 (left) shows that for the 100 % mass.

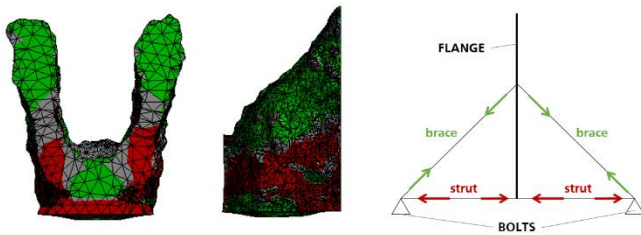


Figure 7 Tensile (green; $>25 \text{ N/mm}^2$) and compressive (red; $<-25 \text{ N/mm}^2$) stresses and the deriving truss model

3.5 Future head plate joints

Taking into account the potentials of Additive Manufacturing the geometry can be changed in such a way that efficiency increases and less material has to be used. The rearrangement of the mass changes the mode of action and almost doubles the load-bearing capacity with the same mass. With only 40 % of the original mass, the same load-bearing capacity is achieved. The optimized head plate could therefore look like Figure 8 in the future.

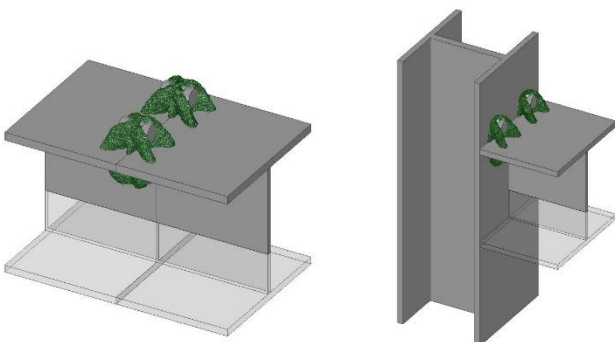


Figure 8 Future 3D-printed beam splice or beam-column-connection

4 Manufacturing

To justify that WAAM is an applicable manufacturing process for such a structure it was printed and tested afterwards. As WAAM is a quite young process there are no sets of parameters available like there are for plastic 3D-printers, for instance [5]. Especially for voluminous structures the former research was very limited [30–32].

4.1 Starting thoughts

Parameters which define the geometry and the behaviour of one welding seam are at least the travel-speed (TS) of the robot arm and the wire-feed-speed (WFS) [21]. For the “CMT Cycle Step” process there are additionally the CMT-regulation, the number of cycles before a pause and the pausing-time. For voluminous structures the distance between each weld and the order of printing influence the out coming structure. This influence is shown in Figure 9 a) and b). If the distance d is equal to the width of the weld w , two separated lines will form. It is easy to see that the distance d should be smaller than the width w . However, if the distance d is too small, the overlapping will lead to an increased height h .

Even if the seams overlap each other, there is still a valley in between the two welds. One way to adjust that problem could be to rotate the welding torch. The pretended result of this is given in Figure 9 c) (blue line). This leads to a smoother surface.

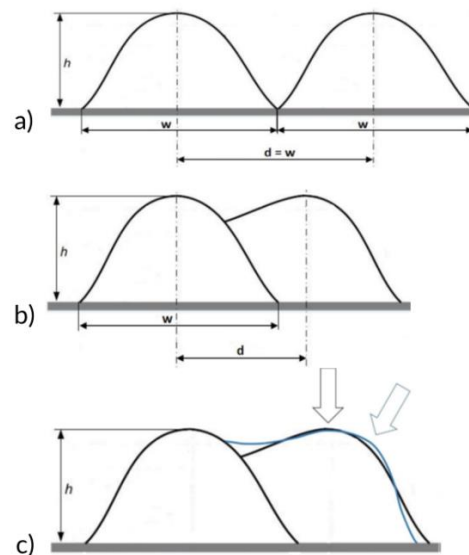


Figure 9 a) + b): relation between weld seam width (w) and distance between the seams (d) c): simulated effect of a rotation of the welding torch © Johanna Dettki

Furthermore, the height of each layer has a direct influence on the accuracy of the final printed structure. Delicate components, which are characterized by small changes in contour, can only be printed with a small layer height.

4.2 Test setup of the parameter study

According to these starting thoughts a printing setup was developed. There were two different distances tested with three different seam widths. Moreover, a rotation of the welding torch (Figure 9 c) was tested for the distance d of 5.0 mm.

In preceding parameter studies the process parameters (WFS, TS, CMT-regulation) for single welding were identified. For all single welds a height h of 1.5 mm was predefined. Table 2 shows the parameter for the test setup. The first printed layer is shown in Figure 10.

Table 2 Test setup of the parameter study

Distance d	5 mm	5 mm	3.5 mm
Specimen no. + seam width w	3 w = 6.5 mm	4 w = 6.5 mm	9 w = 5.0 mm
	2 w = 6.0 mm	5 w = 6.0 mm	8 w = 4.5 mm
	1 w = 5.5 mm	6 w = 5.5 mm	7 w = 4.0 mm
Angle of the welding torch	90°	60°	90°



Figure 10 First printed layer of the parameter study

For each layer the printing path direction is rotated by 90 degrees. This is intended to additionally close the valleys between the seams [30]. Therefore, all odd layers are sliced into welds in x-direction and all even layers into welds in y-direction (see Figure 11).

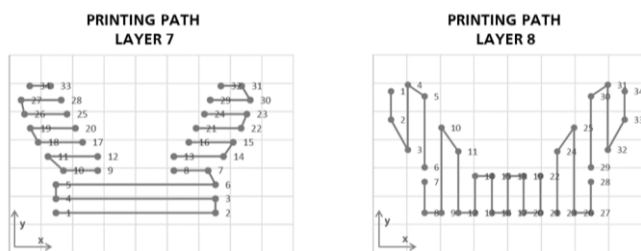


Figure 11 Printing path of two consecutive layers

4.3 Observations during printing

In general, it was possible to produce the desired structure using each set of parameters. However, different combinations lead to advantages and disadvantages. During printing it was noticed that each layer of specimen 9 reached a height of approx. 3 mm due to overlapping and not the intended height of 1.5 mm. What an incorrectly assumed layer height means for the final structure is shown in Figure 12. Therefore, every second layer of specimen 9 was skipped. Additionally, the effect of the perpendicular layer direction, as described above, was compared.

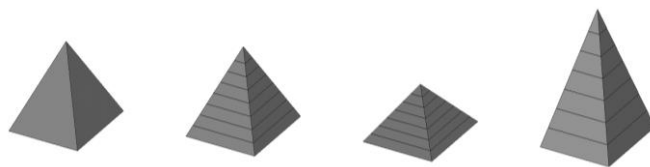


Figure 12 Influence of misconceived layer heights

Contrary to the assumption that a rotated welding torch leads to a smoother surface (Figure 9 c)), the result was not particularly better but led to further difficulties while printing. Since the unknown interplay of weld seam width and distance resulted in different layer heights, the wire sometimes missed the welding seam (see Figure 13).

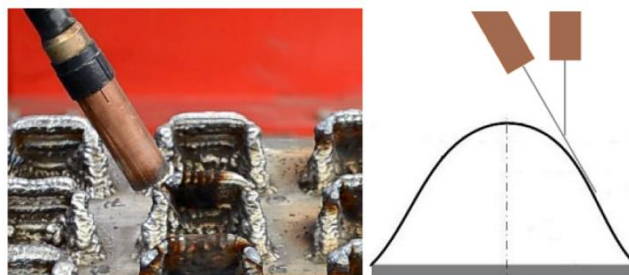


Figure 13 Mismatch of the wire © Johanna Dettki

4.4 Visual examination

In general, the final contour proximity of the nine samples can be considered equivalent. The smaller distance of $d = 3.5$ mm has no significant effect on the accuracy, at least not to the required extent. The best result was achieved by specimen 3. The individual layers show a rather closed surface and the height of the specimen is in accordance with the designed geometry.

In addition to external inspection, the specimens 6, 7 and 8 were cut to identify possible air voids (see Figure 14). Specimen 6 was chosen to investigate the effects of the rotated welding torch. Specimen 9 was chosen because, contrary to the requirement of perpendicular welding, only every second layer and therefore only one welding direction was produced. During the production of specimen 7 there was a change in the process parameters by accident so that instead of 4.0 mm thick welding seams, 3.0 mm thick seams were produced. Here it was interesting to see to what extent the gaps between the seams were closed within the next layer.

While specimens 6 and 9 show a very uniform sectional view, the holes between the welding seams in the second layer of specimen 7 can still be recognized by elongated cracks.



Figure 14 Cut structure

4.5 Evaluation of the functionality

For the production of the specimen the bolt hole was not taken into account, so that it had to be drilled afterwards. Since the first 9 test specimens were partly manufactured with a few days break between the layers and due to some difficulties during the printing process, the surfaces on both, the contact side to the counterpart as well as the contact side of the bolt head are not flat - with the result of a not fully tightened bolt.

In addition, the bolts were difficult to tighten at all. The welding seams protruded into the area provided for tightening, so that the previous intended wrench did not fit. For future designs a certain distance for inaccuracies of the printing process should be included in the optimization. Furthermore, such crucial spots should also be given special attention in the slicing process.

4.6 Evaluation of the load-bearing capacity

Besides the visual examination a first evaluation of the load bearing capacity was made on three specimens. It has to be highlighted that the specimens were the outcome of a test series for finding the right manufacturing strategy, as described above. It should be noted that, in contrast to the numerical model, only one side of the T-stub was printed. Apart from the fact that the specimen just represent half of the previously designed structure (chapter 3), the above mentioned inaccuracies in tightening must be taken into account as well.

These tests served as a justification that the welding parameters lead to acceptable structural behaviour. For this purpose, the specimens were bolted against a stiff bracket and the base plate was extended for the load introduction of the tension force. Because of the half-sided construction the load application is eccentric. An exemplary course of the test can be seen in Figure 15. Due to the eccentric load and the gap between bolt and structure, the specimen rotates and the bolt receives tension and bending. In all three cases, the very thin base plate failed at the point where the load is introduced into the printed specimen. It can be stated that the printed specimen can transmit at least 160 kN (see Table 3 and diagram in Figure 15).

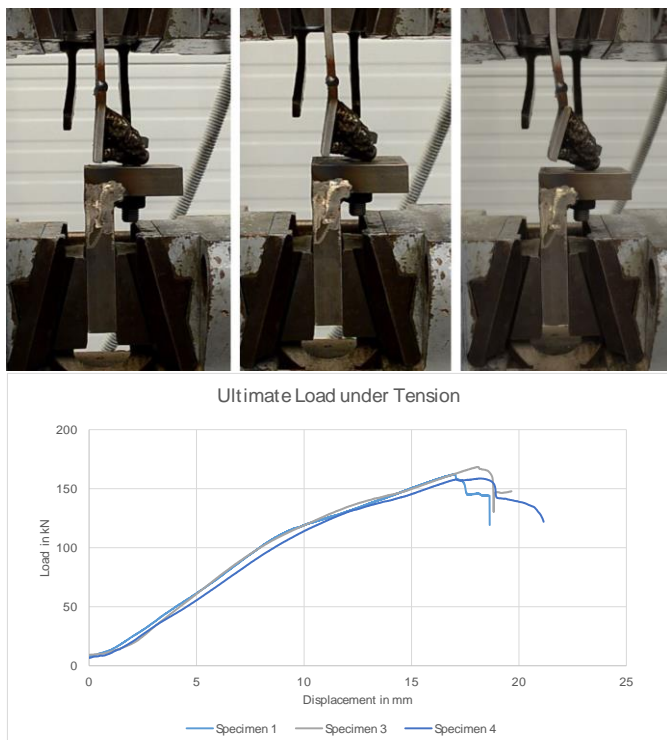


Figure 15 Tension tests and diagram

Table 3 Load bearing capacity tensile tests

Specimen	Load Bearing capacity	Mean value	Standard deviation
1	162.3 kN		
3	168.4 kN	163.1 kN	4.0 kN
4	158.7 kN		

5 Conclusion and outlook

Using the best parameters found a further two specimens were printed. It was checked whether it is possible to weld at the edge of a base plate. In addition, the distance between the two specimens was chosen according to the original distance of the head plate connection. Hereby, a heat influence of the two bodies to each other should also be checked. No such negative effects were observed. The completion of both bodies including the cooling time was 2.5 hours. Afterwards the base plate was cut and the two specimens were bolted together. The result is shown in Figure 16.



Figure 16 Final printed and connected structure

The final print of the completely designed structure and the relating ultimate load tests are still pending. At first, the structure has to be adjusted by allowing more space for the wrench. Also in the bearing area of the bolts the process should be as stable as possible and the roughness of the surface should be as small as possible. Of course the base plate should be chosen according to the design and the structure should be printed on both sides of the plate.

This paper shows how the new production process WAAM can significantly change the shape of structures on the example of a bolted head plate. Therefore, all steps from the original design to the additive manufactured structure are demonstrated, including form finding by using topology optimization, manufacturing with different parameters and a first testing of the manufactured structures.

References

- [1] Shusteff, M.; Browar, A.E.M.; Kelly, B.E. et al.: *One-step volumetric additive manufacturing of complex polymer structures*. In: *Science advances*, Vol. 3 (2017), Iss. 12, eaa05496.
- [2] Buchanan, C.; Gardner, L.: *Metal 3D printing in construction: A review of methods, research, applications, opportunities and challenges*. In: *Engineering Structures* 180 (2019), p. 332-348.

- [3] Strauss, H.: *AM envelope – The potential of additive manufacturing for façade construction*. Delft University of Technology, Faculty of Architecture, Architectural Engineering + Technology Department, Delft, Netherlands, 2012.
- [4] Gebhardt, A.; Kessler, J.; Thurn, L.: *3D printing – Understanding additive manufacturing*. Hanser Publishers, Munich, 2019.
- [5] Feucht, T.; Lange, J.; Erven, M.: *3-D-Printing with Steel: Additive Manufacturing of Connection Elements and Beam Reinforcements*. In: *ce/papers 3* (2019), 3-4, p. 343-348.
- [6] Erven, M.; Feucht, T.; Lange, J. et al.: *Numerische und experimentelle Untersuchungen von Knoten im konstruktiven Stahlbau*. In: DVS (ed.): *DVS Congress 2019, DVS-Berichte Band 355*. DVS Media GmbH, Düsseldorf, 2019, p. 287-294.
- [7] Greitemeier, D.: *Untersuchung der Einflussparameter auf die mechanischen Eigenschaften von additiv gefertigtem TiAl6V4*, Springer Fachmedien Wiesbaden GmbH, Doctoral Thesis, 2016.
- [8] Frazier, W.E.: *Metal Additive Manufacturing: A Review*. In: *Journal of Materials Engineering and Performance* 23 (2014), Vol. 6, p. 1917-1928.
- [9] WAAMMat Team: *WAAM Technology* October 2015. Cranfield university, Cranfield, 2015.
- [10] Filomeno, M.; Stewart, W.: *Wire+arc additive manufacturing vs. traditional machining from solid: a cost comparison*, 1, April 2015.
- [11] Feldmann, M.; Kühne, R.; Citarelli, S. et al.: *3D-Drucken im Stahlbau mit dem automatisierten Wire Arc Additive Manufacturing*. In: *Stahlbau* 88 (2019), Vol. 3, p. 203-213.
- [12] Bergmann, J.-P.; Henckell, P.; Reimann, J. et al.: *Grundlegende wissenschaftliche Konzepterstellung zu bestehenden Herausforderungen und Perspektiven für die Additive Fertigung mit Lichtbogen*, Düsseldorf, March 2018.
- [13] Hartke, M.; Günther, K.; Bergmann, J.P.: *Untersuchung zur geregelten, energiereduzierten Kurzlichtbogentechnik als generatives Fertigungsverfahren*. In: DVS (ed.): *DVS Congress 2014, DVS-Berichte Heft 306*. DVS Media GmbH, Düsseldorf, 2014, p. 98-102.
- [14] Laghi, V.; Palermo, M.; Gasparini, G. et al.: *Experimental results for structural design of Wire-and-Arc Additive Manufactured stainless steel members*. In: *Journal of Constructional Steel Research* (2019), p. 105858.
- [15] Laghi, V.; Palermo, M.; Tonelli, L. et al.: *Tensile properties and microstructural features of 304L austenitic stainless steel produced by wire-and-arc additive manufacturing*. In: *The International Journal of Advanced Manufacturing Technology* 106 (2020), 9-10, p. 3693-3705.
- [16] Bruckner, J.: *Schweißpraxis aktuell: CMT-Technologie – Cold Metal Transfer – ein neuer Metall-Schutzgas-Schweißprozess*. Fronius International GmbH, WEKA-Praxislösungen, WEKA-Media, Kissing, 2013.
- [17] Fronius AG: *Cold Metal Transfer*, Wels, Österreich, 2011.
- [18] Posch, G.; Chladil, K.; Chladil, H.: *Material properties of CMT–metal additive manufactured duplex stainless steel blade-like geometries*. In: *Welding in the World* 61 (2017), Vol. 5, p. 873-882.
- [19] Kühne, R.; Feldmann, M.; Citarelli, S. et al.: *3D printing in steel construction with the automated Wire Arc Additive Manufacturing*. In: *ce/papers 3* (2019), 3-4, p. 577-583.
- [20] Feucht, T.; Lange, J.; Waldschmitt, B. et al.: *Welding Process for the Additive Manufacturing of Cantilevered Components with the WAAM*. In: da Silva, L.F.M.; Martins, P.A.F.; El-Zein, M.S. (ed.): *Advanced Joining Processes, Advanced Structured Materials*. Springer Singapore, Singapore, 2020, p. 67-78.
- [21] Almeida, P.M.S.: *Process control and development in wire and arc additive manufacturing*. Cranfield, Cranfield university, Doctoral Thesis, 2012.
- [22] Lange, J.; Knaack, U.; Feucht, T. et al.: *3-D gedruckte Fußgängerbrücke aus Stahl*. In: Bischoff, M.; Scheven, M.V.; Oesterle, B. (ed.): *Berichte der Fachtagung Baustatik – Baupraxis 14*: 23. und 24. März 2020, Universität Stuttgart, p. 215-222.
- [23] Zoetemeijer, P.: *A design method for the tension side of statically loaded, bolted beam-to-column connections*. In: *Heron* 20 (1974), Vol. 1.
- [24] Kulak, G.L.; Fisher, J.W.; Struik, J.H.A.: *Guide to design criteria for bolted and riveted joints*. Wiley, New York, 1987.
- [25] EN 1993-1-8: *Eurocode 3: Design of steel structures – Part 1-8: Design of joints*. May 2005.
- [26] Ungermann, D.; Puthli, R.; Ummenhofer, T. et al.: *Eurocode 3 Bemessung und Konstruktion von Stahlbauten – Band 2 : Anschlüsse : DIN EN 1993-1-8 mit Nationalem Anhang : Kommentar und Beispiele*. Bauforumstahl e.V.; Bundesingenieurkammer; Deutscher Ausschuss für Stahlbau et al., Beuth Kommentar, Beuth; Ernst & Sohn, Berlin, 2015.
- [27] Bendsøe, M.P.; Sigmund, O.: *Topology optimization – Theory, methods and applications*, Engineering online library, Springer, Berlin, 2004.
- [28] Harzheim, L.: *Strukturoptimierung – Grundlagen und Anwendungen*. Verlag Europa-Lehrmittel, s.l., Haan-Gruiten, Germany, 2014.
- [29] Ali, Y.; Steinerstauch, D.; Günther, K. et al.: *Additive Fertigung von 3D-Verbundstrukturen mittels MSG-Schweißen*. In: DVS (ed.): *DVS Congress 2016, DVS-Berichte Band 327*. DVS Media GmbH, Düsseldorf, 2016, p. 75-80.
- [30] Ding, D.: *Process planning for robotic wire ARC additive manufacturing*. In: *University of Wollongong Thesis Collection 1954-2016* (2015).
- [31] Ding, D.; Pan, Z.; Cuiuri, D. et al.: *A tool-path generation strategy for wire and arc additive manufacturing*. In: *The International Journal of Advanced Manufacturing Technology* 73 (2014), 1-4, p. 173-183.
- [32] Li, Y.; Han, Q.; Zhang, G. et al.: *A layers-overlapping strategy for robotic wire and arc additive manufacturing of multi-layer multi-bead components with homogeneous layers*. In: *The International Journal of Advanced Manufacturing Technology* 96 (2018), 9-12, p. 3331-3344.

